



Aalborg Universitet

**AALBORG UNIVERSITY**  
DENMARK

## **A Quantum Lightning Search Algorithm-Based Fuzzy Speed Controller for Induction Motor Drive**

Hannan, Mahammad A.; Ali, Jamal Abd; Hussain, Aini; Hasim, Fazida Hanim; Amirulddin, Ungku Anisa Ungku; Uddin, Mohammad Nasir; Blaabjerg, Frede

*Published in:*  
IEEE Access

*DOI (link to publication from Publisher):*  
[10.1109/ACCESS.2017.2778081](https://doi.org/10.1109/ACCESS.2017.2778081)

*Publication date:*  
2017

*Document Version*  
Publisher's PDF, also known as Version of record

[Link to publication from Aalborg University](#)

*Citation for published version (APA):*

Hannan, M. A., Ali, J. A., Hussain, A., Hasim, F. H., Amirulddin, U. A. U., Uddin, M. N., & Blaabjerg, F. (2017). A Quantum Lightning Search Algorithm-Based Fuzzy Speed Controller for Induction Motor Drive. *IEEE Access*, 6, 1214-1223. <https://doi.org/10.1109/ACCESS.2017.2778081>

### **General rights**

Copyright and moral rights for the publications made accessible in the public portal are retained by the authors and/or other copyright owners and it is a condition of accessing publications that users recognise and abide by the legal requirements associated with these rights.

- Users may download and print one copy of any publication from the public portal for the purpose of private study or research.
- You may not further distribute the material or use it for any profit-making activity or commercial gain
- You may freely distribute the URL identifying the publication in the public portal -

### **Take down policy**

If you believe that this document breaches copyright please contact us at [vbn@aub.aau.dk](mailto:vbn@aub.aau.dk) providing details, and we will remove access to the work immediately and investigate your claim.

Received October 19, 2017, accepted November 19, 2017, date of publication November 28, 2017, date of current version February 14, 2018.

Digital Object Identifier 10.1109/ACCESS.2017.2778081

# A Quantum Lightning Search Algorithm-Based Fuzzy Speed Controller for Induction Motor Drive

MAHAMMAD A. HANNAN<sup>1</sup>, (Senior Member, IEEE), JAMAL ABD ALI<sup>2</sup>,  
AINI HUSSAIN<sup>3</sup>, FAZIDA HANIM HASIM<sup>3</sup>,  
UNGKU ANISA UNGKU AMIRULDDIN<sup>1</sup>,  
MOHAMMAD NASIR UDDIN<sup>4</sup>, (Senior Member, IEEE),  
AND FREDE BLAABJERG<sup>5</sup>, (Fellow, IEEE)

<sup>1</sup>Electrical Power Engineering, Universiti Tenaga Nasional, 43000 Kajang, Malaysia

<sup>2</sup>South Electrical Station, General Company of Electricity Production, Middle Region, Ministry of Electricity, Baghdad, Iraq

<sup>3</sup>Faculty of Engineering and Built Environment, Universiti Kebangsaan Malaysia, 43600 Bangi, Malaysia

<sup>4</sup>Lakehead University, Thunder Bay, ON P7B 5E1, Canada

<sup>5</sup>Energy Technology, Aalborg University, 9100 Aalborg, Denmark

Corresponding author: Mahammad A. Hannan (hannan@uniten.edu.my)

This work was supported in part by the Universiti Tenaga Nasional Bold Multi-Track Incentive under Grant 10289176/B/9/2017/36 and in part by the Universiti Kebangsaan Malaysia under Grant DIP-2015-012.

**ABSTRACT** This paper presents a quantum lightning search algorithm (QLSA) -based optimization technique for controlling speed of the induction motor (IM) drive. The developed QLSA is implemented in fuzzy logic controller to generate suitable input and output fuzzy membership function for IM drive speed controller. The main objective of this paper is to develop QLSA-based fuzzy (QLSAF) speed controller to minimise the mean absolute error in order to improve the performance of the IM drive with changes in speed and mechanical load. The QLSAF-based speed controller is implemented in simulation model in the MATLAB/Simulink environment and the prototype is fabricated and experimentally tested in a fully integrated DSP for controlling the IM drive system. The experimental results of the developed QLSAF speed controller are compared with the simulation results under different performance conditions. Several experimental results show that there are good agreement of the controller parameters, SVPWM signals, and different types of speed responses and stator currents with the simulation results, which are verified and validated the performance of the proposed QLSAF speed controller. Also, the proposed QLSAF speed controller outperforms other studies with settling time in simulation and in experimental implementation, which validates the controller performance as well.

**INDEX TERMS** Optimization, quantum lightning search algorithm, fuzzy speed controller, IM drive, SVPWM, DSP, validation.

## I. INTRODUCTION

Induction motors (IMs) have been widely used in numerous applications due to its simple structure, low cost, robustness, and a high degree of reliability [1]. The IM drive is configured with power electronic switches which controller can be integrated in DSP, microcontrollers and FPGA [2]–[5]. The performance of the IM drive depends on the type of control strategies used either in scalar or vector to control speed, voltage, current, flux and torque, respectively [6].

During the years, conventional controllers such as PI, PD and PID have been used to control IM drives. However, these controllers have some limitations such as trial-and-error, process upset, needs calculation operations, and mathematical

models [7]–[9]. The fuzzy logic controller (FLC) has been used in scalar and vectors control to control the IM drive with sudden changes of speed and load. This is because FLC does not require a mathematical model and it is capable of handling linear and non-linear systems and generates human logic linguistic rules [10], [11]. However, the performance of FLC depends on its input and output membership functions (MFs), selection of the MFs and fuzzy operational rules. These input and output variables are typically computed by heuristic procedures, which are time-consuming [12].

Different types of pulse width modulation techniques such as sinusoidal PWM (SPWM), hysteresis band PWM (HBPWM), and random pulse width modulation (RPWM)

are generally used to control the switches of the voltage source inverters (VSIs) to regulate the output voltage and frequency of IM drives [13]. However, in some cases, high computational time, harmonic distortion and switching loss may give problems in IM drive control. To address the above problems, space vector pulse width modulation (SVPWM) switching technique is typically used for minimising switching loss and harmonic output signals produced by the inverter [14], [15]. In general, the SVPWM requires complex online computation, which may hinder its real-time implementation. This shortcoming is addressed with an artificial neural network-based SVPWM and an adaptive neural fuzzy inference system (ANFIS) based SVPWM [16], [17]. However, the above mentioned methods require voluminous data and long periods for training and learning the linear and non-linear functions. Thus, an advanced optimal computing method is emerging for controlling the inverter switching signals.

Many researchers have used heuristic optimisation techniques for improving and tuning the control parameters to solve numerous problems and to achieve high performance and efficiency of the IM drives [18]. However, not all heuristic optimisation techniques and their variants provide superior solutions to some specific problems; hence the need for a new heuristic optimisation technique for IM controller is interesting. In hardware implementation, the IM drives are using dSPACE, FPGA, and DSP controllers. The dSPACE and FPGA are rather expensive to implement, and are not applicable for standalone operation [2], [19]. However, DSP is used in many applications because of its fast computational, low power consumption, calculation power and higher density in comparison with other processors.

To overcome the above mentioned problems with controller, optimization and switching signals, a QLSAF speed controller based SVPWM inverter is developed in this paper. The efficacy of the proposed QLSAF speed controller for IM drive is verified by both simulation and experimental results at different operating conditions and also compared with the existing works.

## II. QLSA BASED FUZZY SPEED CONTROLLER

The fuzzy speed controller is used in linear and non-linear control systems due to its performance and also it does not require mathematical model. The controller performance can be further improved by optimizing the control parameters using optimisation techniques. In this research, a quantum wave behaved lightning search algorithm (QLSA) optimization technique is used in a fuzzy speed controller to find the best input and out membership functions (MFs) for the controller. Details of the QLSA and QLSA based fuzzy speed controller (QLSAF) are explained in the following.

### A. QUANTUM LIGHTNING SEARCH ALGORITHM

The concept of QLSA involves in developing a new searching position to obtain the best position for step leaders in a population. In this algorithm, the attraction and the convergence

of each step leader is achieved with a global minimum and searches the best position by relying on the stochastic attractor of the step leaders  $p_j$  as given in the following equation:

$$p_{ij}^t = \frac{a_{ij}^t \cdot P_{ij,best}^t + b_{ij}^t \cdot Gsl_{ij}^t}{c_{ij}^t \cdot SF} \quad (1)$$

for  $i = 1, 2, \dots, N$ ,  $j = 1, 2, \dots, D$ , and  $t = 1, 2, \dots, T$ , where  $N$  is the population size,  $D$  is the problem dimension, and  $T$  is the maximum number of iterations, respectively; for the  $j^{th}$  dimension of step leaders,  $a$ ,  $b$ , and  $c$  are the three uniformly distributed random numbers on the range of (0,1);  $P_{ij,best}^t$  is the best step leader for each population;  $Gsl_{ij}^t$  is the best global step leaders used to obtain the minimum value of the evaluation of the best step leaders, and  $SF$  is scale factor.

In this concept, the quantum behaviour is exhibited in each step leader within its quantum state formulated by a wave function ( $\psi_w$ ), which moves between points,  $P_{ij,best}^t$  and  $Gsl_{ij}^t$ . The wave function, as iteration ( $t + 1$ ), is represented as

$$\psi(P_{ij}^{t+1}) = \frac{1}{\sqrt{L_{ij}^t}} \exp\left(-\left|P_{ij}^t - p_{ij}^t\right|/L_{ij}^t\right) \quad (2)$$

The wave function is calculated within the standard deviation of step leaders based on an exponential distribution. The standard deviation ( $L_{ij}^t$ ) of each step leader is calculated as

$$L_{ij}^t = 2\beta \left| Mbest_j^t - P_{ij}^t \right| \quad (3)$$

where  $\beta$  is the expansion coefficient,  $P_{ij}^t$  represents the personal best position of the step leader  $i$  and  $Mbest_j^t$  is the mean best position of the  $P_{ij,best}^t$  for all step leaders.  $Mbest_j^t$  is calculated as follows:

$$Mbest_j^t = \frac{1}{N} \sum_{i=1}^N P_{ij}^t = \left( \frac{1}{N} \sum_{i=1}^N P_{i1}^t, \frac{1}{N} \sum_{i=1}^N P_{i2}^t, \frac{1}{N} \sum_{i=1}^N P_{i3}^t, \dots, \frac{1}{N} \sum_{i=1}^N P_{ij}^t \right) \quad (4)$$

The expansion coefficient works on the initial and final expansion contractions to control the convergence speed of the algorithms as follows:

$$\beta = \beta_0 + (T - t) \cdot (\beta_1 - \beta_0) / T \quad (5)$$

where  $\beta_0$  is the initial value of the contraction expansion,  $\beta_1$  is the final value of the contraction expansion,  $t$  presents the current iteration number, and  $T$  is the maximum number of iterations.

In each iteration, the distance between step leaders and  $Mbest_j^t$  directs the new position distribution. Thus, the new position of the step leaders,  $P_{ij}^{t+1}$  is updated as follows:

$$P_{ij}^{t+1} = p_{ij}^t \pm \beta \left| Mbest_j^t - P_{ij}^t \right| \ln(1/u_{ij}) \quad (6)$$

The proposed QLSA optimisation method is validated using 14 benchmark functions as employed by several

researchers [20], [21]. In general, the algorithms are tested and validated through functional characteristics such as modality, separability and dimensionality. In this research, 14 benchmark functions of modality and separability are classified into unimodal and separable, unimodal and non-separable, multimodal and separable, and multimodal and non-separable, respectively. All these benchmark functions are used to determine the best solution for the best global minimum, and to observe the algorithm performance consistency. However, there are some problems due to the non-separable, low and high dimensional functions.

### B. QLSA BASED FUZZY STRUCTURE

The QLSA based fuzzy speed controller is structured with three vital elements, namely, input information, objective function, and optimisation limitations [22]. Each element is working for classification and improvement to obtain optimal fuzzy membership functions (MFs). The QLSAF searches space to obtain a best solution by minimising the objective function. However, the input information and the selection of the optimization limitations (constraints) in each generation of the iterative process are manipulated. In this research, the QLSAF controller has been trained, tested and validated for all kinds of sudden changes of operation which occurs in IM such as change in speed and load.

The input data for the QLSAF controller is the number of boundary values for the input and output fuzzy MFs. The numerical values of the MFs boundaries for error and change of error and the output MFs are shown in the matrix as follows:

$$D_{ij} = \begin{bmatrix} X_{11} & X_{12} & X_{13} & \dots & X_{1j} \\ X_{21} & X_{22} & X_{23} & \dots & X_{2j} \\ X_{31} & X_{32} & X_{33} & \dots & X_{3j} \\ \vdots & \vdots & \vdots & \ddots & \vdots \\ X_{i1} & X_{i2} & X_{i3} & \dots & X_{ij} \end{bmatrix} \quad (7)$$

where  $D$  represents the input information to optimisation technique; for  $i = 1, 2, \dots, P, j = 1, 2, \dots, N$ , where  $P$  is the population size,  $N$  is the problem dimension and  $X$  is the variable of MFs. Accordingly, Fig. 1 presents 21 problem dimensions that include 7 MFs for error, change of error, and the output in which 30 populations are used to obtain the best solutions.

The objective function searches for the best value of the controller output to increase system stability. In general, the type of errors in the IM speed drive is uniformly distributed, so the mean absolute error (MAE) is an appropriate objective function to obtain the optimal values of the controller [23]. The MAE function is calculated as follows:

$$MAE = \frac{1}{l} \sum_{m=1}^M |\omega_{rm}^* - \omega_{rm}| \quad (8)$$

where  $l$  represents the sample numbers,  $\omega_{rm}^*$  is the reference rotor speed, and  $\omega_{rm}$  is the rotor speed responsible for motor operation.

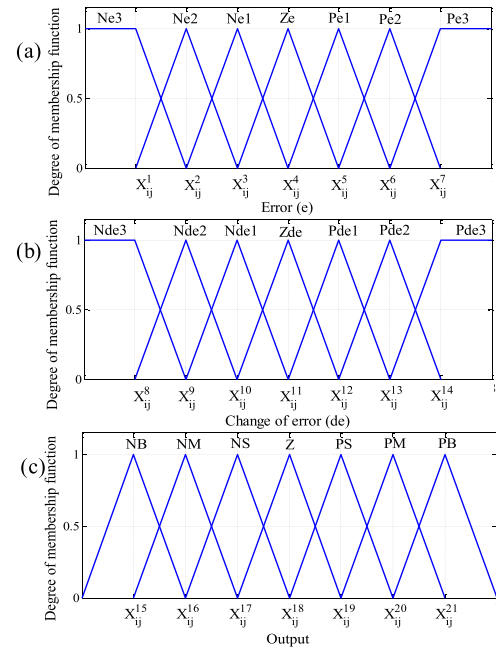


FIGURE 1. Membership functions for (a) error, (b) change of error, and (c) output.

In the QLSAF optimisation technique, all the constraints are implemented to avoid the overlapping between the MFs boundaries. For example, in Fig. 1, the variable  $X_{ij}^2$  should not cross the two variables  $X_{ij}^1$  and  $X_{ij}^3$  to avoid the overlapping that may occur in MFs. The solution of this problem is conducted by imposing limitations as follows:

$$X_{ij}^{P-1} < X_{ij}^P < X_{ij}^{P+1} \quad (9)$$

The main objective of the QLSAF speed controller is to determine the best values of the MF parameters. The controller calculates the step leaders, the initial population, contraction expansion coefficient, mean best position for each projectile to find the best search space for population and the best projectile through the update step leaders.

### C. SPACE VECTOR PWM INVERTER

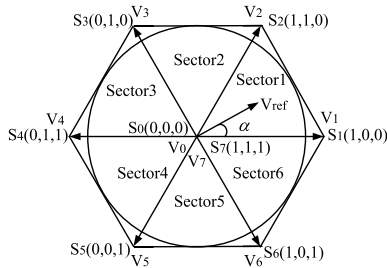
The SVPWM is one of the best switching techniques because of its capability to minimise the harmonic distortion for variable frequency drives [24], [25]. In general, 6-pulse inverter can form eight switch variables as non-zero vectors ( $V_1, V_2, \dots, V_6$ ), and zero vectors ( $V_0, V_7$ ) to represent voltage vectors, switching vectors, output line to neutral voltages, and output line to line voltages as shown in Table 1. The working principle of the SVPWM divides the output wave of the inverter into six sectors in a hexagon shape. Each sector lies between two voltage space vectors while the sector angle is 60 degree apart as shown in Fig. 2 [16].

The SVPWM technique receives a three-phase voltage ( $V_a, V_b$ , and  $V_c$ ) separated by 120 degrees between two phases and converts it into two phases ( $V_\alpha$  and  $V_\beta$ ) with an angle difference of 90 degrees using Clark's transformation. Detail of the SVPWM reference vector, angle,



**TABLE 1.** Switching pattern of voltage space vectors with phase and line voltages.

| Voltage vectors | Switching vectors |       |       | Line to neutral voltage |               |               | Line to line voltage |           |           |
|-----------------|-------------------|-------|-------|-------------------------|---------------|---------------|----------------------|-----------|-----------|
|                 | $S_1$             | $S_2$ | $S_3$ | $V_{an}$                | $V_{bn}$      | $V_{cn}$      | $V_{ab}$             | $V_{bc}$  | $V_{ca}$  |
| $V_0$           | 0                 | 0     | 0     | 0                       | 0             | 0             | 0                    | 0         | 0         |
| $V_1$           | 1                 | 0     | 0     | $2/3 V_{dc}$            | $-1/3 V_{dc}$ | $-1/3 V_{dc}$ | $V_{dc}$             | 0         | $-V_{dc}$ |
| $V_2$           | 1                 | 1     | 0     | $1/3 V_{dc}$            | $1/3 V_{dc}$  | $-2/3 V_{dc}$ | 0                    | $V_{dc}$  | $-V_{dc}$ |
| $V_3$           | 0                 | 1     | 0     | $-1/3 V_{dc}$           | $2/3 V_{dc}$  | $-1/3 V_{dc}$ | $-V_{dc}$            | $V_{dc}$  | 0         |
| $V_4$           | 0                 | 1     | 1     | $-2/3 V_{dc}$           | $1/3 V_{dc}$  | $1/3 V_{dc}$  | $-V_{dc}$            | 0         | $V_{dc}$  |
| $V_5$           | 0                 | 0     | 1     | $-1/3 V_{dc}$           | $-1/3 V_{dc}$ | $2/3 V_{dc}$  | 0                    | $-V_{dc}$ | $V_{dc}$  |
| $V_6$           | 1                 | 0     | 1     | $1/3 V_{dc}$            | $-2/3 V_{dc}$ | $1/3 V_{dc}$  | $V_{dc}$             | $-V_{dc}$ | 0         |
| $V_7$           | 1                 | 1     | 1     | 0                       | 0             | 0             | 0                    | 0         | 0         |


**FIGURE 2.** Space vector diagram used for space vector modulation.

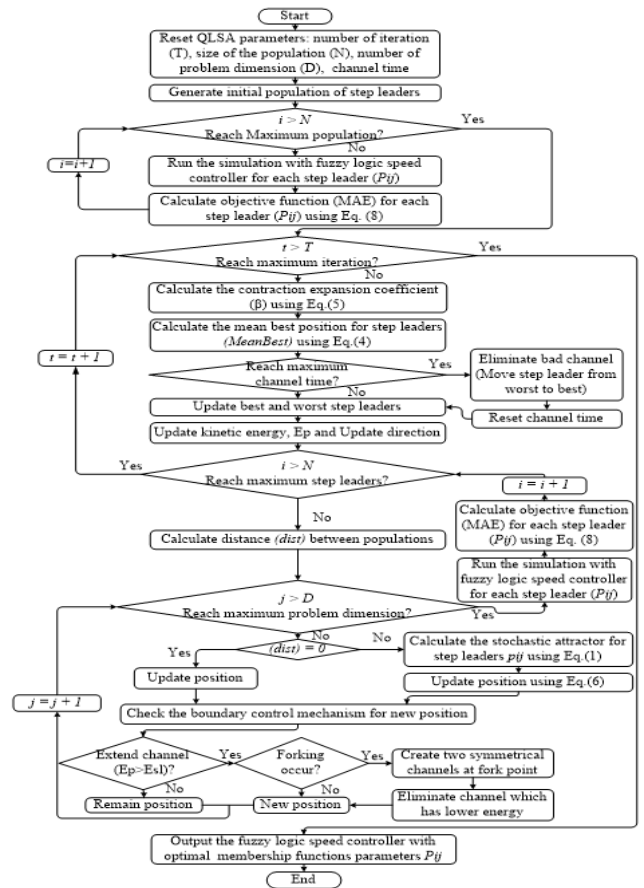
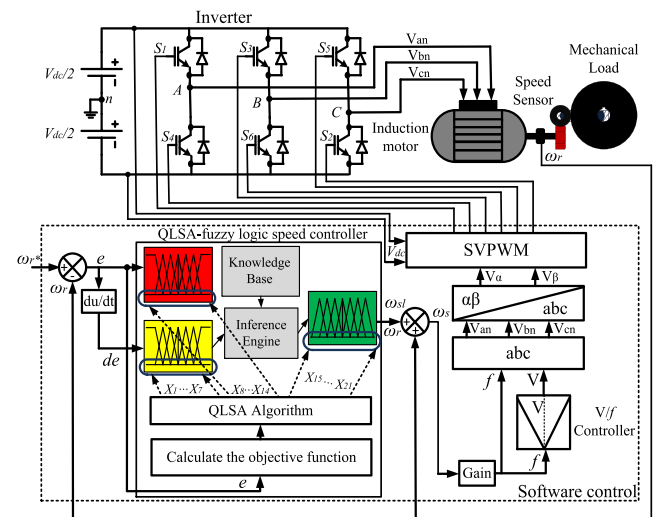
modulation index and switching time durations are explained in [16], [24]–[27].

#### D. ALGORITHMIC FLOW OF THE QLSAF SPEED CONTROLLER

The QLSAF has the fast convergence for solution compared with the other conventional optimisation techniques because it is inspired by natural phenomenon of lightning. However, it has some limitations such as easily trap in local minima, and need the best search for the new position of step leader. The main objective of the QLSAF speed controller is to find the best values of the MFs parameters. The parameters used in these algorithms are the number of iterations ( $T$ ) is 200, and the population size ( $P$ ) is 30. The QLSAF optimisation technique is applied to improve the fuzzy speed controller and implement into IM drive system. Detail of the operational flow of QLSAF speed controller is explained in section II A and II B as shown in Fig. 3.

#### III. SIMULATION MODEL

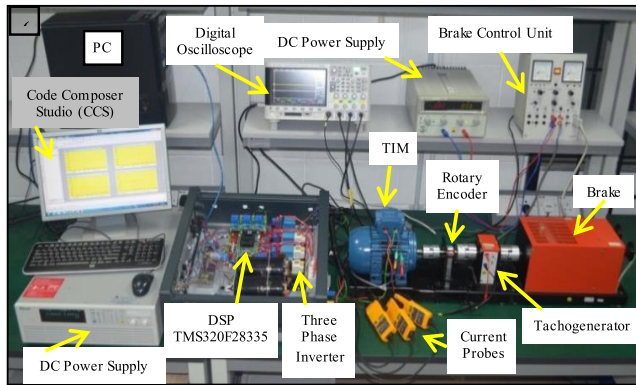
A detailed definition of the parameters is needed to develop a mathematical model for the IM drive in which some parameters are measured and some are obtained from the IM datasheet [28]. In this study, the simulation model includes a QLSAF speed controller, V/f control, SVPWM switching technique, an inverter and an IM, respectively. The v/f control controls the optimal speed of the QLSAF controller and generates amplitude of the stator voltage and operating frequency towards generating the  $V_{alpha}$  and  $V_{beta}$  for the SVPWM input. The SVPWM generates switching


**FIGURE 3.** Proposed QLSA-based optimum fuzzy speed controller design procedure.

**FIGURE 4.** QLSAF speed controller based SVPWM inverter.

signals by comparing the duty ratio ( $T_a$ ,  $T_b$ ,  $T_c$ ) with the triangular signal for the inverter gate drive to deliver AC voltages to the IM. A block diagram of the QLSAF based SVPWM inverter for IM is shown in Fig. 4.

**TABLE 2.** Parameters of the induction motor.

| Parameters                | Values                    |
|---------------------------|---------------------------|
| Nominal power             | 1 HP                      |
| Nominal voltage           | 415 V                     |
| Nominal speed             | 1405 rpm                  |
| Stator resistance         | 13.62 $\Omega$            |
| Rotor resistance          | 5.584 $\Omega$            |
| Stator leakage inductance | 23.23 mH                  |
| Rotor leakage inductance  | 28.72 mH                  |
| Stator leakage reactance  | 7.299 $\Omega$            |
| Rotor leakage reactance   | 9.025 $\Omega$            |
| Mutual reactance          | 190.15 $\Omega$           |
| Nominal frequency         | 50 Hz                     |
| Number of poles           | 4                         |
| Moment of inertia         | 0.00225 Kg.m <sup>2</sup> |



**FIGURE 5.** Experimental setup of MATLAB linked QLSAF speed controlled SVPWM inverter for IM drive prototype implementation.

#### IV. EXPERIMENTAL SETUP

In this paper, a standard 4-pole, 1.0 HP, 50 Hz, and 415 V IM is used. The parameters of the IM are shown in Table 2. A three-phase inverter is used to drive the IM with the switching frequency of 20 kHz and a dead time 5  $\mu$ s. The QLSAF speed controller is implemented using DSP-TM320F28335 controller and received the actual rotor position by an enhanced-quadrature encoder pulse (eQEP). The function of the controller is to allow the real time speed to track the reference speed.

A block diagram of the MATLAB linked QLSAF speed controlled SVPWM inverter setup for the IM drive prototype implementation is shown in Fig. 5. The proposed QLSAF speed controller in the MATLAB/Simulink automatically generates the C-code interfaced by the CCS development environment to build the code for the DSP-TM320F28335 chip to be used for generating the proper switching for the IGBTs. The real rotor speed of the IM is measured by a rotary encoder and the DSP is connected through eQEP. The DSP generates SVPWM signals through the gate pulse generator and then passes them to the gate drives of the IGBTs in the inverter to supply the power needed for the IM drive.

#### V. SIMULATION AND EXPERIMENTAL RESULTS

A comparative analysis is performed between the results obtained from the simulations and experiments to justify the

efficiency of the developed control system. The compared waveforms are the speed controller signals, SVPWM duty ratio, PWMs inverter signals, and the speed response with three-phase stator currents, respectively. Moreover, a detailed comparison is conducted between the existing IM controller and the developed controller.

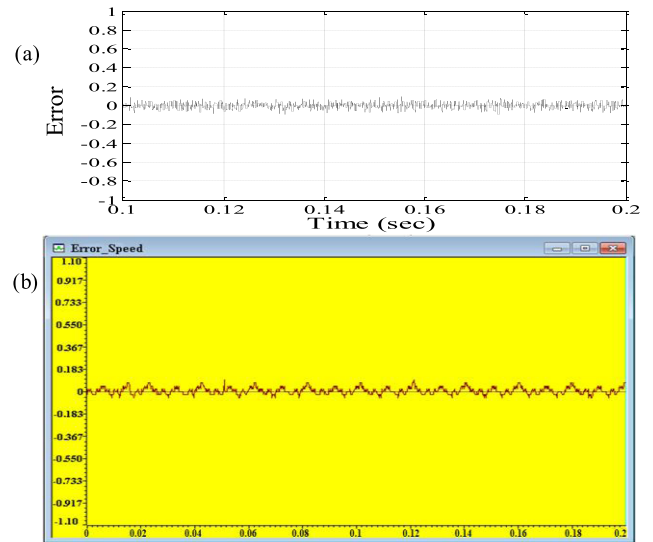


**FIGURE 6.** Speed error signals (a) simulation and (b) experiment.

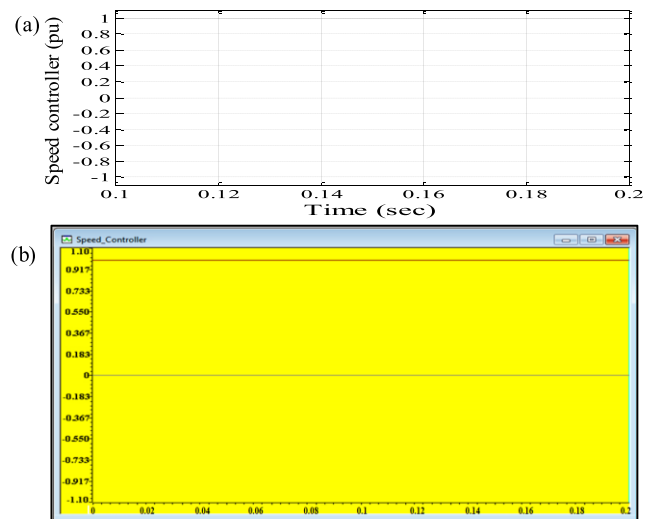


**FIGURE 7.** Speed controller signals (a) simulation and (b) experiment.

#### A. COMPARISON BETWEEN CONTROL PARAMETERS

Fig. 6 to Fig. 9 show comparison between the simulated and experimental controller parameter signals at the full speed case for the IM drive. Fig. 6 shows the simulation and experimental signals for error of rotor speed while the Fig. 7 shows the simulation and experimental signals for the rotor speed of the controller signal. It is noted that the speed controller signals obtained from simulation and experiment are matched each other.

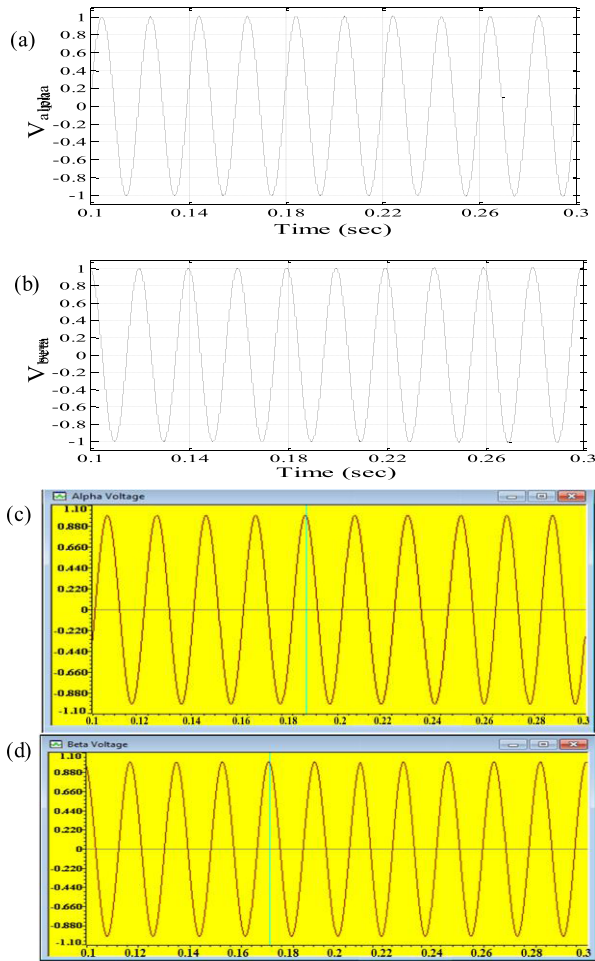


**FIGURE 8.** Alpha and beta voltages for (a)  $V_\alpha$ , (b)  $V_\beta$  for the simulation (c)  $V_\alpha$ , and (d)  $V_\beta$  for the experiment.

Fig. 8 shows the simulation and experimental signals for  $V_\alpha$  and  $V_\beta$ , respectively, which are supplied to SVPWM to generate switching pulses for the inverter switching. Fig. 9 shows the simulation and experimental signals for the duty ratio of only  $T_a$  which is the output of the SVPWM switching techniques. Similarly, the duty ratio of  $T_b$  and  $T_c$  are also perfectly matched with simulation and experiment results. In all cases, the simulation signals are ideally matched with the experimental signals; thereby justifying the performance of the developed controller.

### B. COMPARISON BETWEEN SPEED RESPONSE AND STATOR CURRENTS

A comparison between the speed response and three-phase stator currents waveforms at full speed of the 1 HP motor are obtained from the simulation and experiment as shown in Fig. 10. Fig. 10 (a) shows the simulation results for the speed response and three-phase stator currents. Fig. 10 (b) shows the oscilloscope image of the experimental result for the speed response and the three-phase stator currents in which 0.01 sec/div is used. Moreover, in Fig. 10 (b), the first, second and third channels of the oscilloscope

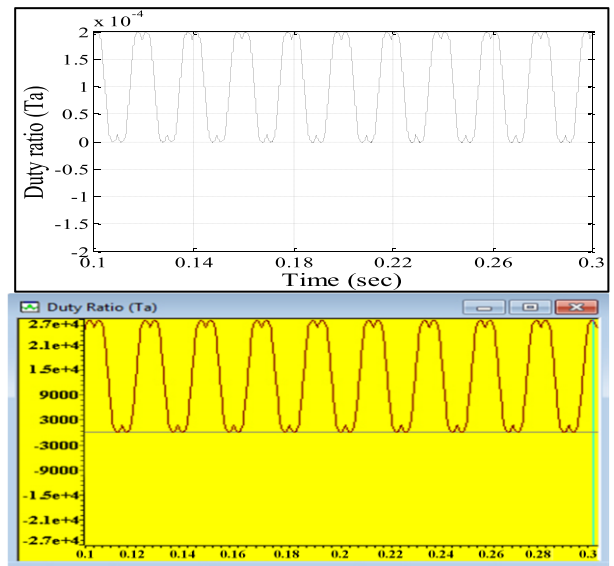


**FIGURE 9.** Duty ratio of the SVPWM technique for (a)  $T_a$  for the simulation and (b)  $T_a$  for the experiment.

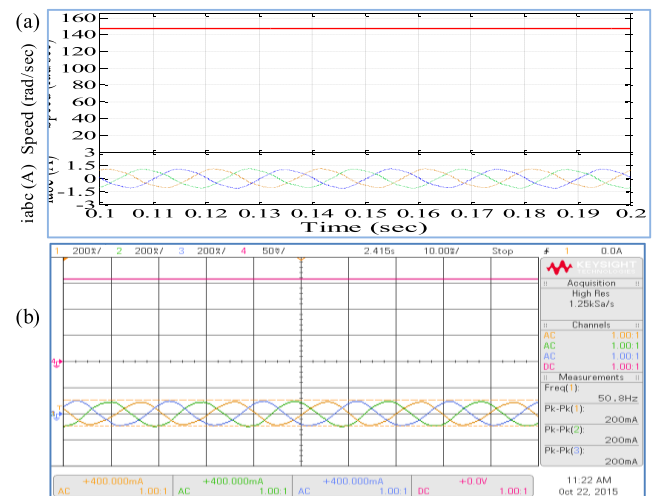


**FIGURE 10.** Full speed response with the three-phase stator currents: (a) simulation and (b) experiment.

represent the stator current for a, b and c-phase, respectively, with 200 mA/Div. The fourth channel represents the speed response with 50 mV/div. It is noticed that the speed response and three-phase stator currents waveforms have a good matching between the simulation and experimental results in terms of speed, frequency and peak current magnitude, respectively.

### C. COMPARISON OF STEP SPEED RESPONSE AND STATOR CURRENTS

The performance of the motor drive during a step response of the speed is determined under constant load (3.2 Nm) and the no-load condition with the speed variable for a short duration. In Fig. 11(a), the simulation results of the speed response is changed at 0.3 sec from speed 74 to 147 rad/sec and again

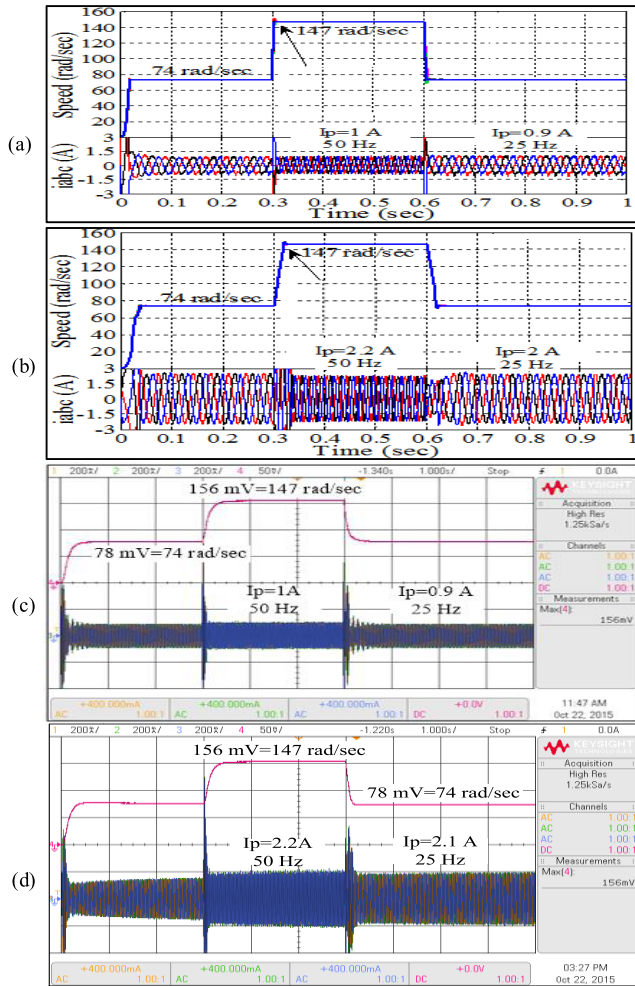


**FIGURE 11.** Step speed responses and stator currents for IM changes from 74 to 147 rad/sec (a) simulation with no load (d) simulation with 3.2 Nm (c) experimental with no load (d) experimental with 3.2 Nm load.

changed to 74 rad/sec at 0.6 sec at no load condition in which peak stator currents are changed from 0.9 A with 25 Hz to 1 A with 50 Hz. Fig. 11(b) shows a similar speed response of Fig. 11(a). However, the stator current is changed from 2.0 A to 2.2 A upon applying 3.2 Nm load condition.

The experimental results of the step speed responses for motor drive under different speeds and load conditions are investigating using the QLSAF speed controller as shown in Fig 11(c) and Fig. 11 (d), respectively. Fig. 11(c) indicates that the speed response of the IM changes at 3 sec from a speed of 74 to 147 rad/sec. The speed returns to 74 rad/sec with no overshoot at 6 sec at the no load condition. By then, the peak stator currents change from 0.9 A with 25 Hz to 1 A with 50 Hz. Fig. 11(d) shows a similar speed response with that shown in Fig. 11 (c). However, the peak stator currents increase from 2.1 A to 2.2 A because of the 3.2 Nm loading. It is worth to mention that the change of speed response and stator currents in both simulation and experimental results are well matched.

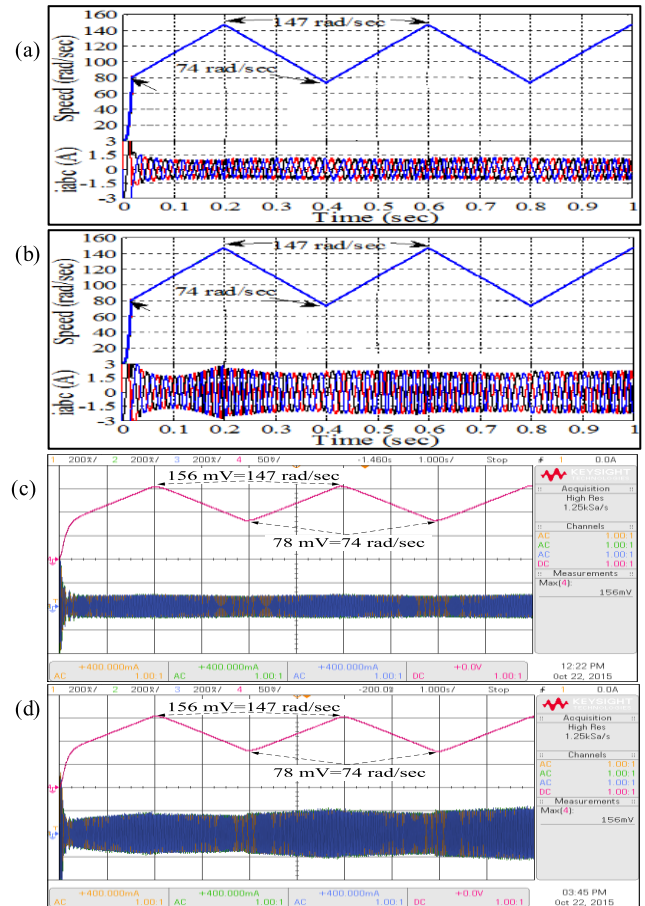


**FIGURE 12.** Ramp speed responses and stator currents for IM changes from 74 to 147 rad/sec (a) simulation with no load (b) with 3.2 Nm load (c) experimental with no load (d) with 3.2 Nm load.

#### D. COMPARISON OF RAMP SPEED RESPONSE AND STATOR CURRENTS

The aim of this validation is to identify the ability of the proposed controller to apply a sudden ramp change in the speed under different load conditions using the QLSAF controller. In Fig. 12(a), the ramp speed response is changed at 0.2 sec from the speed of 147 to 74 rad/sec and continued with the same repeating under no load condition in which the stator current is changed gradually with its frequency. Fig. 12(b) shows a similar ramp speed response of Fig. 12(a). However, stator current is increased at 3.2 Nm load condition.

The ramp tests were conducted experimentally using the proposed QLSAF speed controller for IM drive. The aim of this test is to validate the ability of the proposed speed controller by applying a sudden ramp change under different load conditions. In Fig. 12(c), the ramp speed response is changed at 2 sec from the speed of 147 to 74 rad/sec and continued with the same operation under no load condition in which stator current is changed gradually with it frequency. Fig. 12(d) shows a similar ramp speed response of Fig. 12(c). However, the stator current is increased at 3.2 Nm load



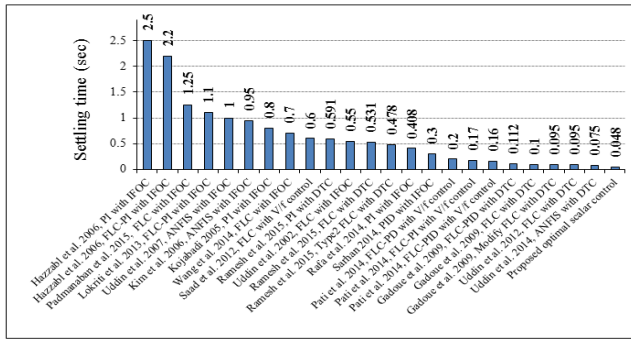


**FIGURE 13.** Comparison of the simulation settling time of proposed optimal control systems with previous works.

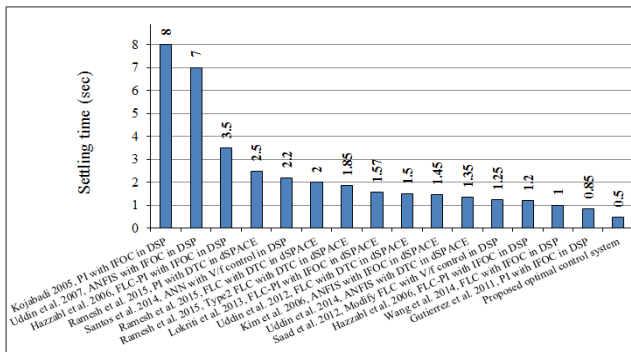


**FIGURE 14.** Comparison of experimental settling time of the proposed control system with previous works.

condition. The obtained results from the prototype implementation are similar with the simulation results, however in scale time of 1 sec/div.

## VI. COMPARATIVE VALIDATION WITH THE EXISTING METHODS

The developed control system for IM is compared with other state-of-the-art control techniques. A total of nineteen reliable studies, similar to the current research in terms of adopted controller technique and system are considered in this comparison [1], [2], [5], [6], [7], [8], [11], [13], [29]–[39]. For example, Ramesh et al. [36] developed a fuzzy logic control based speed estimator for the IM drive. The settling time is one of the most important parameters in justifying the controller performance. Fig. 13 and Fig. 14 show comparison of the settling time between the existing and proposed controller both in simulations and experiments, respectively. The proposed control system for the IM outperforms the techniques of the other studies with a settling time of 0.048 sec in the simulation as shown in Fig. 13. However, the proposed control system settling time in the experimental implementation is 0.5 sec, which is the best among all the other existing systems as shown in Fig. 14.

## VII. CONCLUSIONS

A novel QLSA optimisation based fuzzy speed controller (QLSAF) is presented to solve constrained optimisation problems of the IM drive systems. In this controller, the scalar

control is optimised for the input and output MFs of the fuzzy speed controller by minimising the MAE objective function and the error of the speed response. To evaluate the efficiency and reliability of the QLSAF, 14 benchmark functions are tested with various characteristics in evaluating the optimization algorithm. The real-time model for the optimised QLSAF speed controller is developed in the MATLAB/SIMULINK environment to generate the SVPWM switching signals for the inverter gate drive. Thereafter, the developed controller is implemented in hardware by using DSP controller board TMS320F28335 for a prototype IM drive system. The developed control system model is compiled, converted into C-code using CCS and automatically linked to the real-time TMS320F28335 processor control board. The simulation and experimental results on the control signals such as error and change of error of the rotor speed,  $\alpha$ - $\beta$  voltages, duty ratio of the SVPWM switching signals, different types of speed responses and stator currents are compared for validation and verification. It is found that the control signals of the simulation and the experiment are well matched. The settling times of the proposed QLSAF controller outperforms the other studies. Thus, the proposed QLSAF controller could be a potential candidate for real time IM drive systems.

## REFERENCES

- [1] T. H. dos Santos, A. Goedtel, S. Augusto, O. da Silva, and M. Suetak, "Scalar control of an induction motor using a neural sensorless technique," *Electr. Power Syst. Res.*, vol. 108, pp. 322–330, Mar. 2014.
- [2] C. M. F. S. Reza, M. D. Islam, and S. Mekhilef, "A review of reliable and energy efficient direct torque controlled induction motor drives," *Renew. Sustain. Energy Rev.*, vol. 37, pp. 919–932, Sep. 2014.
- [3] S. Pan, J. Pan, and Z. Tian, "A shifted SVPWM method to control DC-link resonant inverters and its FPGA realization," *IEEE Trans. Ind. Electron.*, vol. 59, no. 9, pp. 3383–3391, Sep. 2012.
- [4] A. Anuchin and Y. Vagapov, "Instructional laboratory for practical investigation of electric drive control," *IET Circuits, Devices Syst.*, vol. 11, no. 4, pp. 344–351, 2017.
- [5] G. Wang, R. Yang, and D. Xu, "DSP-based control of sensorless IPMSM drives for wide-speed-range operation," *IEEE Trans. Ind. Electron.*, vol. 60, no. 2, pp. 720–727, Feb. 2013.
- [6] H. Sarhan, "Efficiency optimization of vector-controlled induction motor drive," *Int. J. Adv. Eng. Technol.*, vol. 7, no. 3, p. 666, 2014.
- [7] A. Hazzab, I. K. Bousserhane, M. Zerbo, and P. Sicard, "Real time implementation of fuzzy gain scheduling of PI controller for induction motor machine control," *Neural Process. Lett.*, vol. 24, no. 3, pp. 203–215, 2006.
- [8] S. Lekhchine, T. Bahi, and Y. Soufi, "Indirect rotor field oriented control based on fuzzy logic controlled double star induction machine," *Int. J. Elect. Power Energy Syst.*, vol. 57, pp. 206–211, May 2014.
- [9] J. Lee, M. Jin, and P. Chang, "Variable PID gain tuning method using backstepping control with time-delay estimation and nonlinear damping," *IEEE Trans. Ind. Electron.*, vol. 61, no. 12, pp. 6975–6985, Dec. 2014.
- [10] M. Suetake, I. N. da Silva, and A. Goedtel, "Embedded DSP-based compact fuzzy system and its application for induction-motor v/f speed control," *IEEE Trans. Ind. Electron.*, vol. 58, no. 3, pp. 750–760, Mar. 2011.
- [11] S. Rafa, A. Larabi, L. Barazane, M. Manceur, N. Essounbouli, and A. Hamzaoui, "Implementation of a new fuzzy vector control of induction motor," *ISA Trans.*, vol. 53, no. 3, pp. 744–754, 2014.
- [12] K. Premkumar and B. V. Manikandan, "Speed control of brushless DC motor using bat algorithm optimized adaptive neuro-fuzzy inference system," *Appl. Soft Comput.*, vol. 32, pp. 403–419, Jul. 2015.
- [13] N. Saad and M. Arrofiq, "A PLC-based modified-fuzzy controller for PWM-driven induction motor drive with constant V/Hz ratio control," *Robot. Comput. Integr. Manuf.*, vol. 28, no. 2, pp. 95–112, 2012.
- [14] E. A. R. E. Ariff, O. Dordevic, and M. Jones, "A space vector PWM technique for a three-level symmetrical six-phase drive," *IEEE Trans. Ind. Electron.*, vol. 64, no. 11, pp. 8396–8405, Nov. 2017.



- [15] C. Charumit and V. Kinnarees, "Discontinuous SVPWM techniques of three-leg VSI-fed balanced two-phase loads for reduced switching losses and current ripple," *IEEE Trans. Power Electron.*, vol. 30, no. 4, pp. 2191–2204, Apr. 2015.
- [16] G. Durgasukumar and M. K. Pathak, "Comparison of adaptive neuro-fuzzy-based space-vector modulation for two-level inverter," *Int. J. Electr. Power Energy Syst.*, vol. 38, no. 1, pp. 9–19, 2012.
- [17] W. Liang, J. Wang, P. C. K. Luk, W. Fang, and W. Fei, "Analytical modeling of current harmonic components in PMSM drive with voltage-source inverter by SVPWM technique," *IEEE Trans. Energy Convers.*, vol. 29, no. 3, pp. 673–680, Sep. 2014.
- [18] J. A. Ali, M. A. Hannan, A. Mohamed, and M. Abdolrasol, "Fuzzy logic speed controller optimization approach for induction motor drive using backtracking search algorithm," *Measurement*, vol. 78, pp. 49–62, Jan. 2016.
- [19] S. Gdaim, A. Mtibaa, and M. F. Mimouni, "Design and experimental implementation of DTC of an induction machine based on fuzzy logic control on FPGA," *IEEE Trans. Fuzzy Syst.*, vol. 23, no. 3, pp. 644–655, Jun. 2015.
- [20] H. Shareef, A. A. Ibrahim, and A. H. Mutlag, "Lightning search algorithm," *Appl. Soft Comput.*, vol. 36, pp. 315–333, Nov. 2015.
- [21] Y. Yuan, H. Xu, B. Wang, and X. Yao, "A new dominance relation-based evolutionary algorithm for many-objective optimization," *IEEE Trans. Evol. Comput.*, vol. 20, no. 1, pp. 16–37, Feb. 2016.
- [22] J. A. Ali, M. A. Hannan, and A. Mohamed, "A novel quantum-behaved lightning search algorithm approach to improve the fuzzy logic speed controller for an induction motor drive," *Energies*, vol. 8, no. 11, pp. 13112–13136, 2015.
- [23] T. Chai and R. R. Draxler, "Root mean square error (RMSE) or mean absolute error (MAE)?—Arguments against avoiding RMSE in the literature," *Geoscientific Model Devices*, vol. 7, no. 3, pp. 1247–1250, 2014.
- [24] Z. Xueguang, Z. Wenjie, C. Jiaming, and X. Dianguo, "Deadbeat control strategy of circulating currents in parallel connection system of three-phase PWM converter," *IEEE Trans. Energy Convers.*, vol. 29, no. 2, pp. 406–417, Jun. 2014.
- [25] B. Jacob and M. R. Baiju, "Space-vector-quantized dithered sigma-delta modulator for reducing the harmonic noise in multilevel converters," *IEEE Trans. Ind. Electron.*, vol. 62, no. 4, pp. 2064–2072, Apr. 2015.
- [26] B. K. Bose, *Power Electronics and Motor Drives: Advances and Trends*. San Diego, CA, USA: Academic, 2010.
- [27] N. V. Naik, A. Panda, and S. P. Singh, "A three-level fuzzy-2 DTC of induction motor drive using SVPWM," *IEEE Trans. Ind. Electron.*, vol. 63, no. 3, pp. 1467–1479, Mar. 2016.
- [28] *WEG Data 2015*. Accessed: Oct. 12, 2015. [Online]. Available: <http://www.weg.net/my/Products-Services/Electric-Motors/IEC-General-Purpose>
- [29] S. Padmanaban, J. L. Daya, F. Blaabjerg, N. Mir-Nasiri, and A. H. Ertas, "Numerical implementation of wavelet and fuzzy transform ifoc for three-phase induction motor," *Int. J. Eng. Sci Technol.*, vol. 19, no. 1, pp. 96–100, 2016.
- [30] A. Lokriti, I. Salhi, S. Doubabi, and Y. Zidani, "Induction Motor speed drive improvement using fuzzy IP-self-tuning controller: A real time implementation," *ISA Trans.*, vol. 52, no. 3, pp. 406–417, 2013.
- [31] M. N. Uddin and H. Wen, "Development of a self-tuned neuro-fuzzy controller for induction motor drives," *IEEE Trans. Ind. Appl.*, vol. 43, no. 4, pp. 1108–1116, Jul. 2007.
- [32] M. N. Uddin and M. Hafeez, "FLC-based DTC scheme to improve the dynamic performance of an IM drive," *IEEE Trans. Ind. Appl.*, vol. 48, no. 2, pp. 823–831, Mar. 2012.
- [33] M. N. Uddin, Z. R. Huang, and A. B. M. S. Hossain, "Development and implementation of a simplified self-tuned neuro-fuzzy-based IM drive," *IEEE Trans. Ind. Appl.*, vol. 50, no. 1, pp. 51–59, Jan./Feb. 2014.
- [34] S.-M. Kim and W.-Y. Han, "Induction motor servo drive using robust PID-like neuro-fuzzy controller," *Control Eng. Pract.*, vol. 14, no. 5, pp. 481–487, 2006.
- [35] H. M. Kojabadi, "Simulation and experimental studies of model reference adaptive system for sensorless induction motor drive," *Simul. Model. Pract. Theory*, vol. 13, no. 6, pp. 451–464, 2005.
- [36] T. Ramesh, A. K. Panda, and S. S. Kumar, "Type-2 fuzzy logic control based MRAS speed estimator for speed sensorless direct torque and flux control of an induction motor drive," *ISA Trans.*, vol. 57, pp. 262–275, Jul. 2015.
- [37] S. Pati, M. Patnaik, and A. K. Panda, "Comparative performance analysis of fuzzy PI, PD and PID controllers used in a scalar controlled induction motor drive," in *Proc. Int. Conf. Circuit, Power Comput. Technol. (ICCPCT)*, 2014, pp. 910–915.
- [38] S. M. Gadoue, D. Giaouris, and J. W. Finch, "Artificial intelligence-based speed control of DTC induction motor drives—a comparative study," *Electr. Power Syst. Res.*, vol. 79, no. 1, pp. 210–219, 2009.
- [39] C. A. Gonzalez-Gutierrez, J. Rodriguez-Resendiz, G. Mota-Valtierra, E. A. Rivas-Araiza, J. D. Mendiola-Santibañez, and R. Luna-Rubio, "A PC-based architecture for parameter analysis of vector-controlled induction motor drive," *Comput. Electr. Eng.*, vol. 37, no. 6, pp. 858–868, 2011.



**MAHAMMAD A. HANNAN** (M'10–SM'17)

received the B.Sc. degree in electrical and electronic engineering from the Chittagong University of Engineering and Technology, Chittagong, Bangladesh, in 1990, and the M.Sc. and Ph.D. degrees in electrical, electronic, and systems engineering from the National University of Malaysia, in 2003 and 2007, respectively. He was the Professor of Intelligent Systems in the National University of Malaysia. He is currently a Professor

of intelligent systems with the Department of Electrical Power Engineering, College of Engineering, Universiti Tenaga Nasional, Malaysia. His research interests include intelligent controllers, power electronics, hybrid vehicles, energy storage systems, image and signal processing, and artificial intelligence.



**JAMAL ABD ALI** received the B.Sc. degree in

electrical and electronics engineering from the University of Technology, Iraq, in 2005, the M.Sc. degree in power engineering from the College of Electrical and Electronic Engineering Techniques, Iraq, in 2010, and the Ph.D. degree in electrical and electronic engineering from the Department of Electrical, Electronics and Systems Engineering, Universiti Kebangsaan Malaysia in 2016.

He is currently with the South Electrical Station, General Company of Electricity Production Middle Region, Ministry of Electricity, Baghdad, Iraq. His research interests include intelligent controllers for induction motors using optimization methods to enhance performance efficiency.



**AINI HUSSAIN** received the B.Sc. degree in electrical

engineering from Louisiana State University, USA, the M.Sc. degree from the University of Manchester Institute of Science and Technology, U.K., and the Ph.D. degree from the Universiti Kebangsaan Malaysia. She is currently a Professor with the Department of Electrical, Electronics, and Systems Engineering, Faculty of Engineering and Built Environment, Universiti Kebangsaan Malaysia. Her research interests include decision

support systems, machine learning, pattern precognition, signal, and image processing.



**FAZIDA HANIM HASIM** received the B.Sc. and

M.Sc. degrees from Carnegie Mellon University, Pittsburgh, in 2003 and 2005, and the Ph.D. degree in electrical, electronic, and systems engineering in 2012 from the Universiti Kebangsaan Malaysia, Malaysia. She is currently a Senior Lecturer with the Department of Electrical, Electronics, and Systems Engineering, Faculty of Engineering and Built Environment, Universiti Kebangsaan Malaysia. Her research interests include intelligent

systems, multi-agent systems, multirotor, and VLSI design.



**UNGKU ANISA UNGKU AMIRULDDIN** received the B.Eng. degree in electrical and electronics engineering from the Imperial College, U.K. in 2001, and the Ph.D. degree in electrical and electronics engineering from the University of Nottingham, U.K., in 2005. She is currently an Associate Professor with the Department of Electrical Power Engineering, College of Engineering, Universiti Tenaga Nasional, Malaysia. Her research interests include induction motor drive, inverter controller, and intelligent systems.



**MOHAMMAD NASIR UDDIN** (S'99–M'00–SM'04) received the B.Sc. and M.Sc. degrees in electrical and electronic engineering from the Bangladesh University of Engineering and Technology, Dhaka, Bangladesh, in 1993 and 1996, respectively, and the Ph.D. degree in electrical engineering from the Memorial University of Newfoundland, St. John's, NF, Canada, in 2000. He is currently a Professor with the Department of Electrical Engineering, Lakehead University,

Thunder Bay, ON, Canada, where he is engaged in teaching and research. His research interests include power electronics, electric motor drives, and applications of neural networks.

...



**FREDE BLAABJERG** (S'86–M'88–SM'97–F'03) received the Ph.D. degree in power electronics from Aalborg University, Aalborg, Denmark. He was with ABB-Scandia, Randers, Denmark, from 1987 to 1988. He is currently a Professor with the Aalborg University, Denmark. His current research interests include power electronics and its applications, such as in wind turbines, PV systems, reliability, harmonics, and adjustable speed drives. He received the 18 IEEE Prize Paper Awards,

the IEEE PELS Distinguished Service Award in 2009, the EPE-PEMC Council Award in 2010, the IEEE William E. Newell Power Electronics Award in 2014, and the Villum Kann Rasmussen Research Award in 2014. He was the Editor-in-Chief of the IEEE TRANSACTIONS ON POWER ELECTRONICS from 2006 to 2012. He was nominated in 2014, 2015, and 2016 by Thomson Reuters in the most 250 cited Researchers in Engineering in the world.